1991A&A...243..445R

Astron. Astrophys. 243, 445–452 (1991)

ASTRONOMY AND ASTROPHYSICS

An investigation of polarization produced by circumstellar dust envelopes

A.V. Raveendran

Indian Institute of Astrophysics, Bangalore-560034, India

Received July 24, accepted September 1, 1990

Abstract. Numerical computations show that: (i) the polarimetric behaviour of carbon stars is inconsistent with the scattering by graphite grains, (ii) the radial pulsation of the star does not significantly change the net polarization produced by an envelope, (iii) the envelope geometry has very little effect on the normalized wavelength dependence, and (iv) if the illuminating star has a non-uniform surface brightness distribution, circumstellar grain scattering produces not only significant changes in the normalized wavelength dependence of polarization but also polarization changes across spectral features.

Key words: polarization – late-type stars – variable stars – circumstellar matter

1. Introduction

Many late-type variables exhibit intrinsic linear polarization which often varies quasi-periodically (Dyck 1968; Kruszewski et al. 1968; Dyck & Jennings 1971; Dyck & Sanford 1971; Serkowski 1971; Shawl 1975a). There are two main mechanisms usually invoked to explain the intrinsic polarization of late-type stars in general. Harrington (1969) has shown that the light emerging from the limb of a star would be highly polarized due to Raleigh scattering by molecules or atoms if the Planck function has a steep gradient in the atmosphere. However, for a net observable polarization, photospheric asymmetry should be present and the proposed sources of asymmetry are non-radial pulsation of the star, variation of temperature over the surface and the presence of giant convection cells (Harrington 1969; Schwarzchild 1975). The other suggested mechanism is the scattering by molecules or dust grains in an extended asymmetric circumstellar envelope (Kruszewski et al. 1968; Shawl 1975b; Daniel 1978).

The available computational models of polarization (Shawl 1975b; Daniel 1978, 1980; Simmons 1982) deal with the scattering of isotropically emitted light from a stellar point source by particles distributed in an envelope around it, and most of the polarization results presented in the literature are for axisymmetric envelopes with uniform particle densities.

Calculations of radiative transfer in dust envelopes by Rowan-Robinson & Harris (1983a, 1983b) indicate high inner shell temperatures (~ 1000 K), especially for carbon stars, suggesting the presence of dust grains in the close vicinity of the objects. The amount of polarization produced will depend on the angle subtended by the source at the scatterer. For the case of steady mass outflow, the density falls as the inverse square of the radial distance (Gilman 1972), and hence the contribution by the dust grains close to the star to the net observed polarization will be substantial. Hence, it is expected that the varying size of the star as it pulsates might modify the observed polarization, such that, when the object is most compact, the polarization produced by an envelope would be the largest (Coyne & Magalhaes 1979). A quantitative analysis of the changes in polarization as a result of the changes in the physical size of the star is lacking.

The identification of grains in the envelope presents a major difficulty because of the inverse nature of the problem involved. However, polarization models of Shawl (1975b) show that a rough qualitative agreement with the observations of several objects can be obtained by using the standard candidates for dust grains (silicates, graphites, etc.) with a suitable choice of their sizes.

The processes leading to the asymmetry of the envelopes around most of the late-type objects, that is needed for a net polarization to be observed, are still open questions. Asymmetric mass ejection, similar to that proposed for the case of R Lep (Raveendran & Rao 1989), may be one such mechanism. Another mechanism may be a mass ejection associated with non-radial pulsations. Rotation might play a role in the production of an axisymmetric envelope. A net polarization can also result from the illumination of a spherical cloud by a star with non-uniform surface brightness (Doherty 1986), and may be one of the mechanisms operating in some of the objects.

In what follows the above aspects of polarization produced by grain scattering in a circumstellar envelope are discussed from a theoretical point of view, using numerical modeling.

2. Mathematical formulation

The following assumptions are made: (i) the light emitted by the star is unpolarized, (ii) the grains are spherically symmetric, and (iii) the single scattering approximation holds good. The last assumption implies that each particle sees only the direct light from the star, and it is not in serious conflict with the observations of the objects under consideration in view of the low optical depths derived for them (Rowan-Robinson & Harris 1983b)

Consider an element of area $\mathrm{d}S$ on the stellar surface and a volume element $\mathrm{d}V$ in the envelope at a distance r. If $\eta(a)$ is the corresponding particle size distribution, the Stokes parameters in terms of the intensity of light scattered by the particles in $\mathrm{d}V$ will be given by (neglecting limb-darkening)

$$\mathrm{d}I_{\mathrm{sca}} = (1/2\,KD^2)\int_a (i_1(a)+i_2(a))\frac{I\cos\theta}{r^2}\,\mathrm{e}^{-(\tau_1-\tau_2)}\,\eta(a)\,\mathrm{d}a\;\mathrm{d}S\;\mathrm{d}V$$

© European Southern Observatory • Provided by the NASA Astrophysics Data System

1991A&A...243..445R

$$dQ=(1/2KD^2)\int_a (i_1(a)-i_2(a))\frac{I\cos\theta}{r^2}e^{-(\tau_1-\tau_2)}$$
$$\times\eta(a)da\,dS\,dV\cos 2\phi$$
$$dU=(1/2KD^2)\int_a (i_1(a)-i_2(a))\frac{I\cos\theta}{r^2}e^{-(\tau_1-\tau_2)}$$
$$\times\eta(a)da\,dS\,dV\sin 2\phi$$
$$V=0.0,$$

where $K=(2\pi/\lambda)$, is the wave number, I, the intensity normal to dS, θ, the angle between the normal and the line joining centres of dS and dV, τ_1, the optical depth between dS and dV, τ_2, the optical depth between the scatterer and the observer, D, the distance between the observer and the scatterer, and i_1 and i_2 are the intensity functions defined by van de Hulst (1957). ϕ is the azimuth of the scattering plane projected over the sky, and the factors $\cos 2\phi$ and $\sin 2\phi$ appear because it is necessary to refer the contribution arising from each part of the envelope to the same coordinate system. Integrations over the star and the envelope provide the net required quantities. The elemental optical depth is obtained from

$$d\tau=\int_a \pi a^2\,\eta(a)\,Q_{ext}(a)\,da\,dl,$$

where dl is the element of path length and $Q_{ext}(a)$, the extinction efficiency. Usually, one is interested in the normalized Stokes parameters defined as $(I_{sca}, Q, U, V)/I_{total}$. If the intensity of direct light received from the star is denoted by I_{dir}, then

$$I_{total}=I_{dir}+I_{sca},$$

with

$$I_{dir}=(1/D^2)\int I\cos\theta\, e^{-\tau}dS,$$

where θ is the angle between the normal to dS and the line of sight and τ, the optical depth along the line of sight. The integration is done over the visible hemisphere.

3. Computer program

We have developed a computer program in Fortran to calculate the polarization produced by grain scattering in a circumstellar envelope surrounding a star of finite size. A Cartesian coordinate system is adopted with the positive x-axis along the line of sight, y- and z- axes in the plane of the sky, and the origin coinciding with the centre of the star. The star is assumed to consist of a specified number of source points distributed uniformly across its surface, and the envelope is divided into a specified number of equal volume elements. The basic program to calculate i_1, i_2 and Q_{ext} are adopted from Shah (1977). The radiation from each of the source points scattered by each of the possible volume elements is calculated and then summed over both the source points on the star and the volume elements in the envelope to give the normalized Stokes parameters Q and U. The program reproduces the results of Zellner (1971), Shawl (1975b) and Simmons (1982) when the corresponding parameters are introduced. Since both Q and U are calculated, the specified envelope need not be axisymmetric as assumed in the earlier investigations (Zellner 1971; Shawl 1975b; Daniel 1978, 1980).

4. Computational results

4.1. *Effect of varying size of star*

We have considered a star of radius $R_\star$ surrounded by a circumstellar dust envelope of inner boundary radius R_I where the dust grains start condensing, and have computed the polarization produced by the envelope for various values of $R_\star$. Three different envelope geometries were considered: (a) an ellipsoid of axial ratio $E=3$ with a particle density $\rho=a$ constant, and spheroids with particle density distributions, (b) $\rho(\theta)\propto(1-f\cos\theta)$, and (c) $\rho(\theta)\propto r^{-2}(1-f\cos\theta)$, where f is a constant less than unity, and θ is the angle between the radius vector and the positive/negative z-axis (for points above/below the x–y plane). About 8000 volume elements in the envelope and 130 surface elements on the star were taken for the purpose of computing the polarization produced; on doubling these numbers the net polarization changes by 2.3% and 0.3%, respectively.

The grains were assumed to be of size $a=0.1$ μm and refractive index $m=1.65$ (which corresponds to pure silicates, Simmons 1982). Calculations were made for $\lambda=0.5$ μm, and the optical depth along the equatorial direction in all cases was assumed to be $\tau_N=0.4$. The attenuation of direct and scattered light inside the envelope, and the contribution of scattered light to the total light were neglected while calculating the normalized polarization.

The computations show that the behaviour of normalized polarization is independent of the value of f appearing in the above dust density distributions (b) and (c). In Fig. 1, the normalized polarization ($P_0=1$, for a point source) is plotted against the corresponding ratio ($R_\star/R_I$) of the stellar radius to the inner shell radius of the envelope for the three geometries assumed, and it is clear from the figure that the relative change in polarization depends on the radial distribution of particle density; but the actual change in polarization with variation in the relative size of the star is very small. If the temperatures are sufficiently low for grain formation to start at 3–4 stellar radii (especially, in the case of the red variables), the net change in polarization as a result of changes in the physical size of the star during the pulsation (assuming it to be radial) is only a few percent. It is safe to conclude that there is little direct effect of radial pulsation of the star on the polarization produced by an envelope as a result of its varying size, and that changes in polarization observed in many red variables may be mainly resulting from changes in the number and sizes of the scattering grains.

4.2. *The nature of grains*

In the light of the above results, the star was assumed to be a point source, and the polarization produced by a circumstellar envelope surrounding it was computed for a wide range of grain sizes (single size particles in each case) assuming them to be pure silicates, dirty silicates and graphites, in order to assess their suitability in explaining the mean polarimetric behaviour of red variables. The refractive index for pure silicates was taken to be $m=1.65$ (Simmons 1982) and that for dirty silicates to be $m=1.55-0.1\,i$ (Jones & Merrill 1976). The optical constants for graphite were taken from Wickramasinghe & Guillaume (1965) after correcting for the misprints (some of the values under k are listed as 1.452 instead of 1.425). The density in the envelope was assumed to vary as $\rho(\theta)\propto r^{-2}(1-0.5\cos\theta)$ and about 8000 volume elements were considered in the envelope for computing the polarization produced. The optical depth at $\lambda^{-1}=2.06\,\mu m^{-1}$

© European Southern Observatory • Provided by the NASA Astrophysics Data System

1991A&A...243..445R

was assumed to be $\tau_N = 0.4$ along the x–y plane in all cases. As before, the attenuation of scattered light in the envelope and its contribution to the total light were neglected.

The computed normalized polarization (unity at $\lambda^{-1} = 2.06\,\mu m^{-1}$) for a few grain sizes, which lie close to the observational results, are plotted in Figs. 2–4. The dashed lines in Figs. 2 and 3 represent the mean polarimetric behaviour of the oxygen-rich stars, and the dashed line in Fig. 4 represents that of the carbon stars (Raveendran 1991). A comparison of the results of polarization calculations assuming single scattering with that taking into account multiple scatterings (Daniel 1978) shows that significant disagreement between them occurs only for optical depths $\tau > 0.6$. In all the cases plotted in Figs. 2–4, the optical depths in the wavelength regions considered never exceeded 0.6, thereby making the contribution of multiple scattering insignificant.

Rowan-Robinson & Harris (1983a) have reported that dirty silicates give an excellent fit to the overall IR emission from circumstellar dust shells around oxygen-rich stars, and from Figs. 2 and 3 it is clear that they provide better approximation to the scattering dust grains than pure silicates also in accounting for the polarimetric behaviour. It is clear from Fig. 4 that graphites do not adequately explain the polarimetric behaviour of carbon stars; here it may be mentioned that neither do they adequately

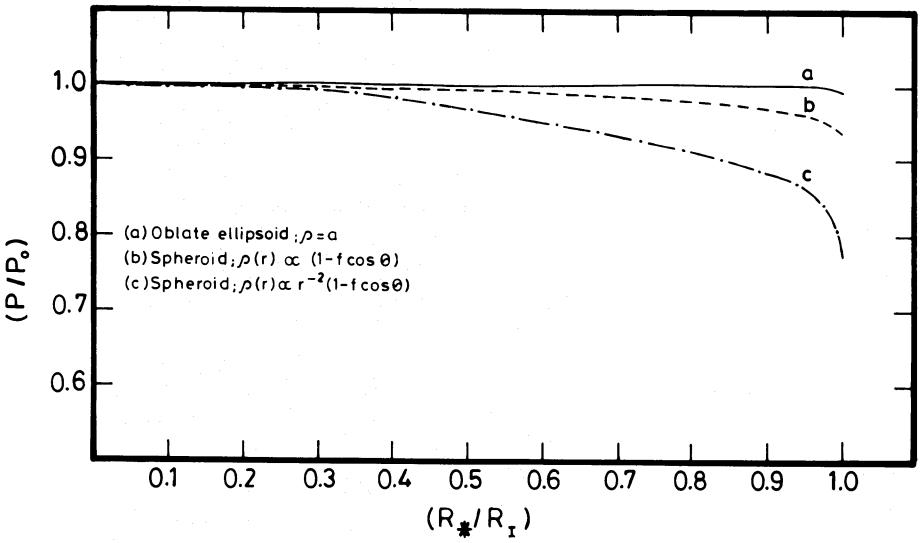

Fig. 1. Plots of the normalized polarization against the corresponding ratio of the stellar to the inner shell envelope radii. The assumed envelope geometries are indicated

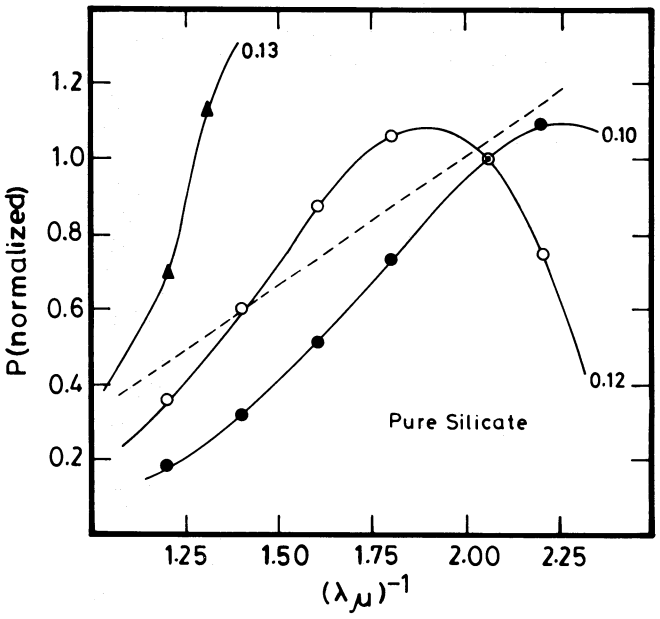

Fig. 2. Plots of the normalized polarization (continuous curves) for pure silicates. The values given next to the curves are the respective grain sizes in microns. The dashed line represents the mean normalized polarimetric behaviour of oxygen-rich stars (see text)

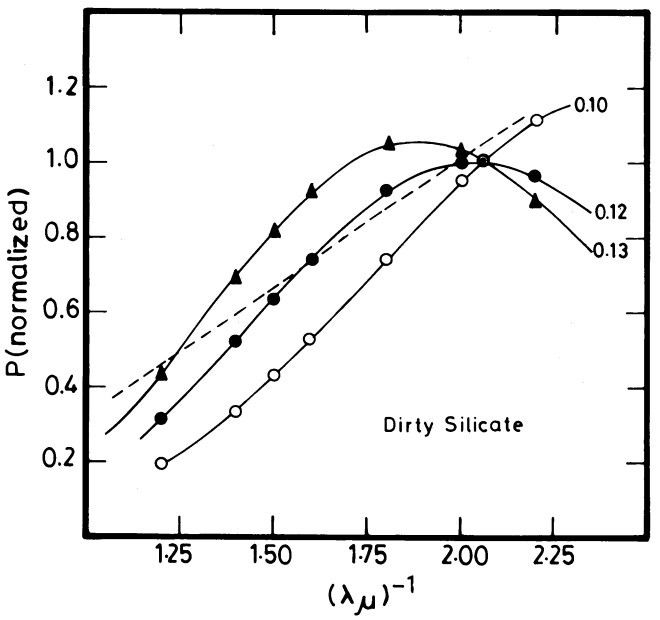

Fig. 3. Plots of the normalized polarization (continuous curves) for dirty silicates. The values given next to the curves are the respective grain sizes in microns. The dashed line represents the mean normalized polarimetric behaviour of oxygen-rich stars (see text)

© European Southern Observatory • Provided by the NASA Astrophysics Data System

1991A&A...243..445R

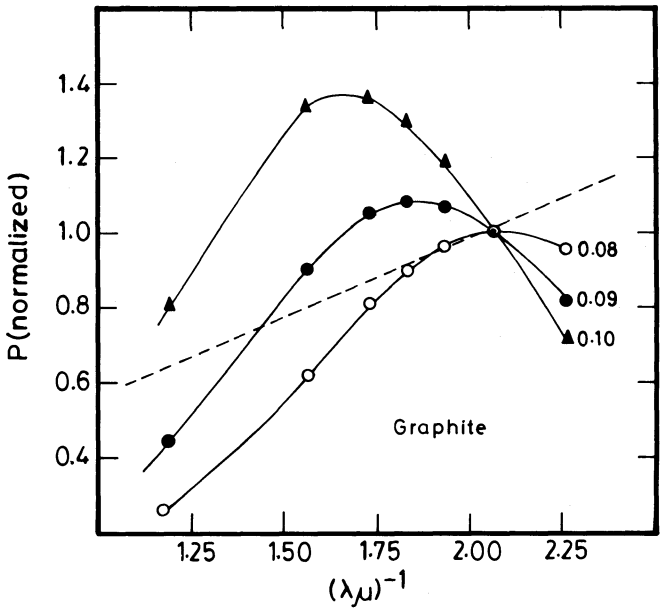

Fig. 4. Plots of the normalized polarization (continuous curves) for graphites. The values given next to the curves are the respective grain sizes in microns. The dashed line represents the mean normalized polarimetric behaviour of carbon stars (see text)

explain the IR spectra of circumstellar dust envelopes around carbon-rich objects (Rowan-Robinson & Harris 1983b). It has been pointed out by Czyzak et al. (1982) that graphite formation in circumstellar envelopes is not a very likely process and carbon grains exist, most likely, in some other form, such as amorphous carbon.

4.3. *Effect of envelope geometry*

In Fig. 5, the polarization, normalized to unity at $\lambda^{-1}=2.06\,\mu$m, is plotted against the corresponding inverse of the wavelength for graphite grains of size $a=0.1\,\mu$m and for the envelope geometries considered in Sect. 4.1; the figure also contains the results for two other envelope geometries: (i) a double sector and (ii) a spherical wedge, both of constant density throughout. In all cases the optical depth along the x–y plane is normalized to $\tau=0.4$ at $\lambda=0.485\,\mu$m. The results for the last two cases are presented by Shawl (1975b) also. It is found that the normalized wavelength dependence of polarization is independent of the value of f appearing in (b) and (c) of the assumed geometries of Sect. 4.1. The close resemblances in the shapes of the various curves plotted in Fig. 5 clearly indicate that the envelope geometries have very little effect on the normalized wavelength dependence of polarization, as already pointed out by Shawl (1975b).

4.4. *Effect of non-uniform surface brightness*

For simplicity, as shown in the inset of Fig. 6, the illuminating star was considered to have three brightness zones – an equatorial zone characterized by a temperature T_E and two polar zones (about y-axis), both characterized by a temperature T_P. The boundaries of polar zones are obtained by rotating a radius vector at an angle θ with the $+$ve/$-$ve y-axis. The dust envelope was assumed to be spherical with the density $\rho(r)\propto r^{-2}$, and the scattering grains to be pure silicates ($m=1.65$) of size $a=0.1\,\mu$m. The optical depth at $\lambda=0.5\,\mu$m along the radial direction was normalized to $\tau_0=0.4$, and the ratio of the inner dust shell radius to the stellar radius was taken as $(R_\star/R_I)=0.2$. The contribution of scattered light to the total light was taken into account while calculating the net polarization produced; but the attenuation of both direct and scattered light inside the envelope was neglected. Computations of polarization at $\lambda=0.5\,\mu$m were made for different areas of polar zones (A_P), first by keeping $T_E=5000$ K and varying T_P, and then keeping $T_P=5000$ K and varying T_E. In Figs. 6 and 7, the net polarization produced by the envelope is plotted against the fractional area $(A_P/4\pi R_\star^2)$ of the polar zones. About 500 surface elements both in the polar and equatorial regions and about 7000 volume elements in the envelope were

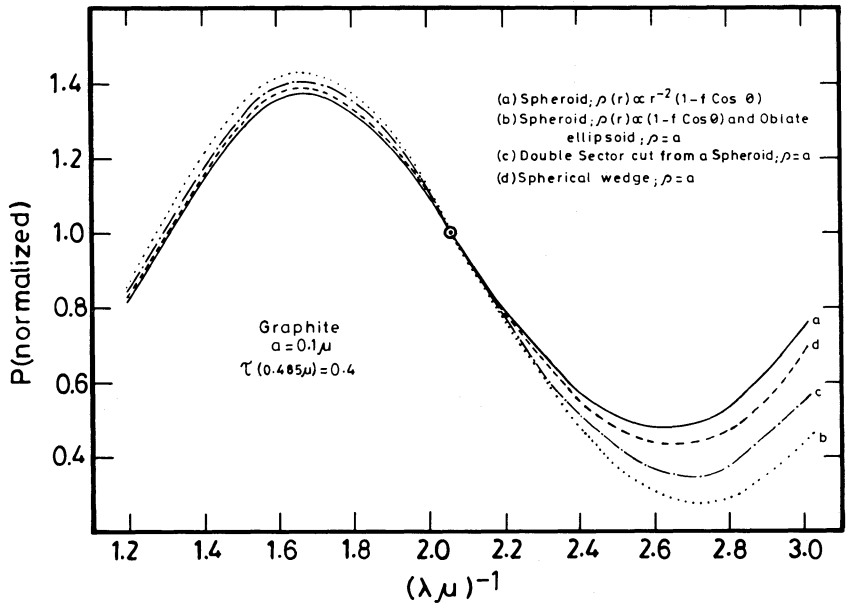

Fig. 5. Plots of normalized wavelength dependence of polarization for different envelope geometries

© European Southern Observatory • Provided by the NASA Astrophysics Data System

1991A&A...243..445R

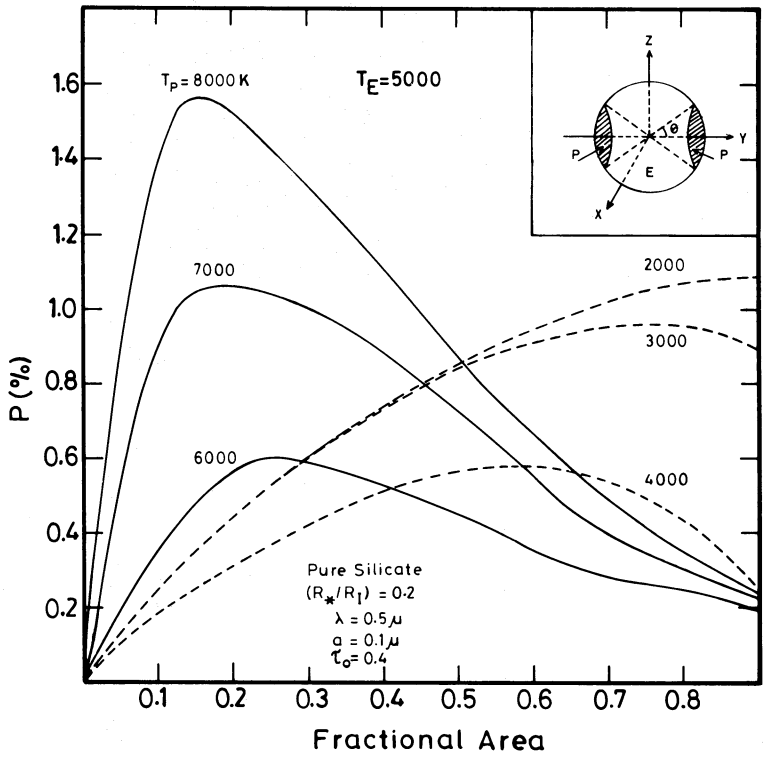

Fig. 6. Plots of linear polarization produced against the corresponding fractional area of the polar zones (shown in the inset of the figure) for different polar zone temperatures (T_p). The temperature of the equatorial zone is taken as T_E = 5000 K

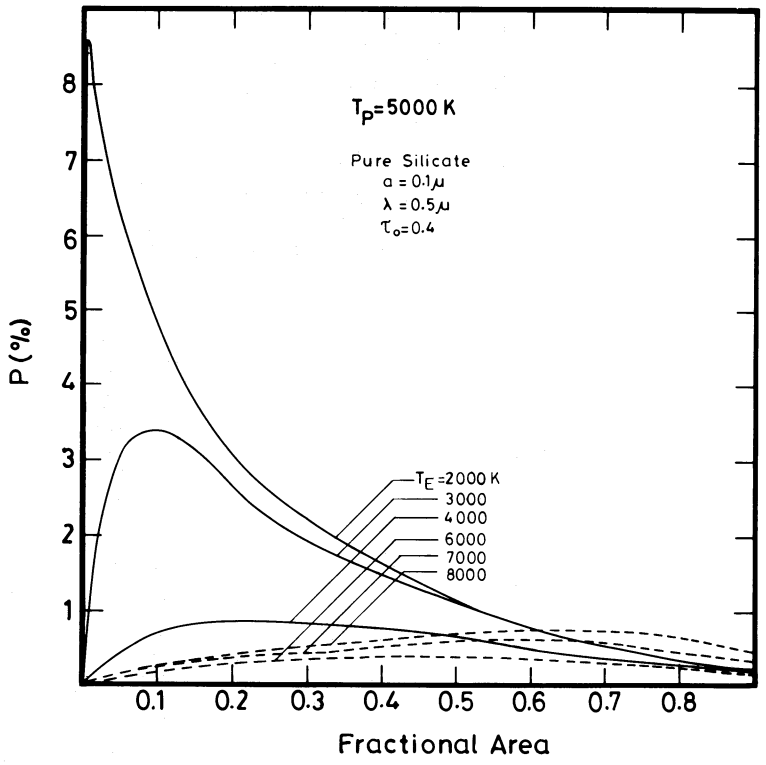

Fig. 7. Plots of linear polarization produced against the corresponding fractional area of the polar zones (see the inset of Fig. 6) for different equatorial zone temperatures (T_E). The temperature of the polar zones is taken as T_p = 5000 K

considered; the net polarization computed by this combination for $T_P = T_E$ is found to be $\leq 0.04\%$ in each case.

From Figs. 6 and 7, it is clear that the polarization produced by a hotter zone at the limb is larger than that produced by a zone of the same temperature and equivalent area about a plane passing through the centre; for example, a 5000 K temperature zone covering an area of $\sim 10\%$ of the stellar surface produces a polarization $\sim 5\%$ when present at the poles, whereas the net polarization produced by an equatorial zone of an equivalent area is $< 1\%$, the ambient surface temperature being 2000 K.

© European Southern Observatory • Provided by the NASA Astrophysics Data System

1991A&A...243..445R

To see the effect of non-uniform surface brightness on the wavelength dependence, the net polarization, produced at wavelengths 0.35, 0.45, 0.50, 0.70, and 0.90 μm, was computed for the geometry described above and shown in the inset of Fig. 6. The fractional area of the polar zones was taken as 0.13. The grains were assumed to be of size $a=0.6$ μm and the optical depth at $\lambda=0.5$ μm was normalized to $\tau_0=0.2$. Calculations were made for two cases of equatorial zone temperatures, $T_E=2000$ K and 4000 K, and the results are presented in Fig. 8 where the polarization, normalized to unity at $\lambda^{-1}=2.0\,\mu m^{-1}$, is plotted against the inverse of the wavelength. From the figure it is found that the shape of the normalized $P(\lambda)$ curve depends on the relative values of T_P and T_E, the less the difference the steeper the curve towards UV; for large differences between them all the curves converge to the same. Larger changes occur in the blue-UV region than in the red-IR region. The shape of the curve also depends on the relative position of the hotter zone with respect to the centre of the projected stellar disc. The normalized $P(\lambda)$ curves, corresponding to two different positions of the hotter zones, are shown in Fig. 9. The curve is less steeper towards UV when the hotter zone is close

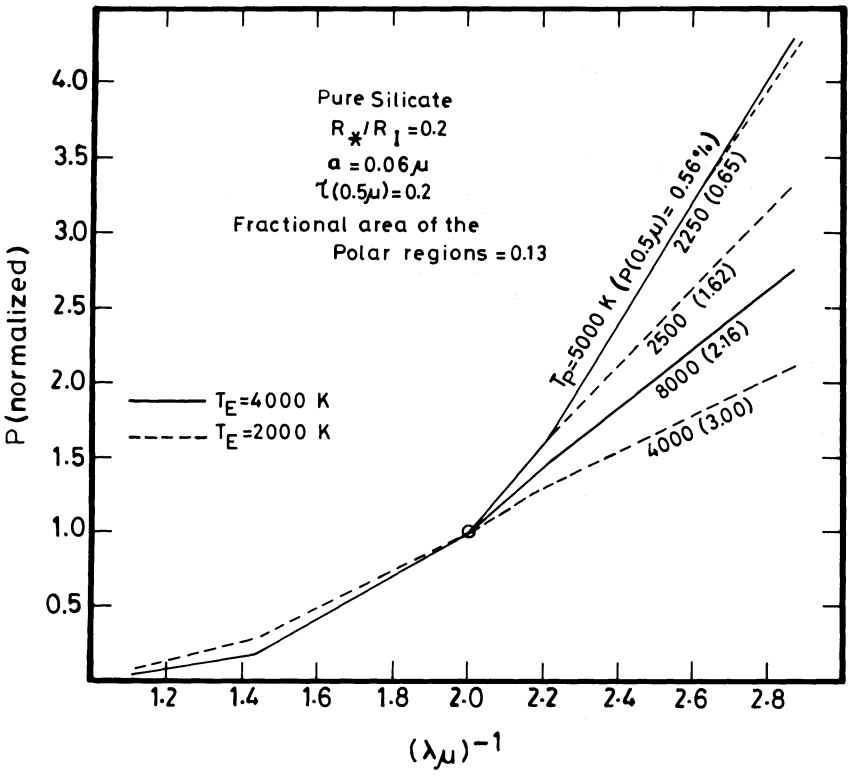

Fig. 8. Plots of normalized wavelength dependence of polarization for different combinations of polar and equatorial zone temperatures (see the inset of Fig. 6). The solid lines represent the cases for $T_E=4000$ K and the dashed lines for the case $T_E=2000$ K. The values inside the brackets indicate the percentage of linear polarization at the normalizing wavelength $\lambda=0.5$ μm and the numbers outside the brackets, the polar zone temperatures T_p

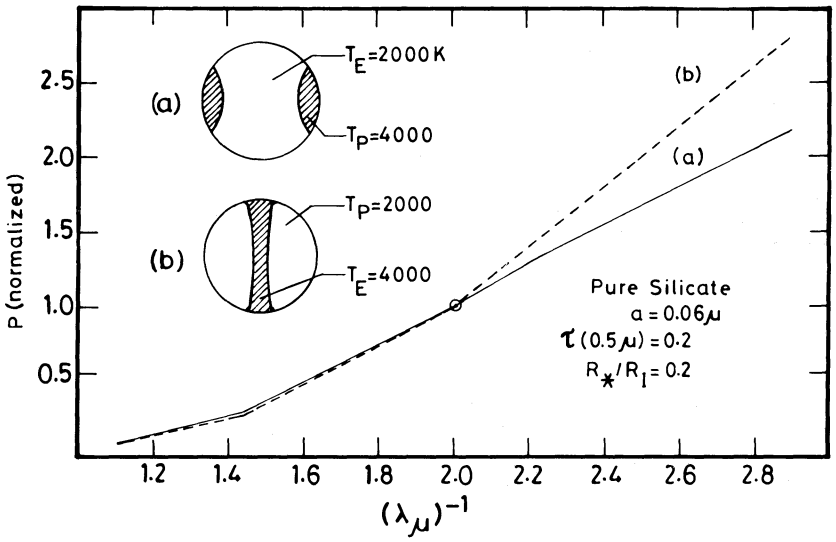

Fig. 9. Plots of normalized wavelength dependence for two positions of the hotter zone which are also shown in the figure. The fractional areas in the two cases (a) and (b) are 0.13, and 0.09, respectively

© European Southern Observatory • Provided by the NASA Astrophysics Data System

1991A&A...243..445R

to the limb (case a) than when it is about the centre of the projected stellar disc (case b). The fractional areas in the two cases are 0.13 and 0.09, respectively.

In the cases considered above, a net polarization at each wavelength results because of the differences in the emergent fluxes from the polar and equatorial zones at that wavelength. With changes in temperature, the flux in the blue-UV region changes more rapidly than that in the red-IR region, thereby producing larger changes in polarization in the blue-UV region.

Figure 10 is a plot of the polarization at $\lambda = 0.5$ μm against the corresponding polar zone temperature T_P for the case of an equatorial temperature $T_E = 2000$ K. The ratios of the blackbody fluxes $[F(T_P)/F(T_E)]$ are also indicated along the x-axis. It is seen from the figure that for a given polar zone area the polarization does not increase monotonously with the ratio of emergent fluxes from the polar and equatorial zones, but rather stays at a nearly constant value after $[F(T_P)/F(T_E)] \sim 50$.

The results presented above have some important implications on the polarization produced, especially by red variables. Polarization changes across spectral features, observed in several cool objects, have been, usually, attributed to photospheric mechanisms (Landstreet & Angel 1977; Coyne & McLean 1979; Boyle et al. 1986). If different temperature zones exist on the stellar surface, possibly arising from non-spherical atmospheric shocks or non-radial pulsations, one would expect changes in polarization across the spectral features, because the net polarization produced at any wavelength as a result of circumstellar grain scattering depends on the distribution of emergent flux across the surface at that wavelength. This may be yet another mechanism which produces polarization changes across spectral features. The large dispersion seen in the UV region of the normalized $P(\lambda)$ curve of M-type Mira variables has been ascribed to differences in the grain size distributions (Dyck & Sanford 1971). The present calculations show that any change in the brightness distribution of the illuminating star also has larger effects in the UV region than in the red-IR region of the normalized $P(\lambda)$ curve. More detailed model calculations are needed along the lines considered here.

5. Conclusions

Numerical computations show that the changes in the net polarization produced by an envelope due to changes in the size of a star, as a result of radial pulsation, is not significant. However, in objects that show polarization variation coupled with the pulsation, other effects such as changes in the number and sizes of scattering grains may be occurring as a result of the changes in temperature during the pulsation cycle. The mean polarimetric behaviour of oxygen-rich stars is found to be more consistent with the scattering by grains of dirty silicate than by pure silicate grains. It is also found that the polarimetric behaviour of red carbon stars is inconsistent with the scattering by graphite grains, suggesting the existence of carbon grains in the envelopes around them in some other forms, such as amorphous carbon. Polarization changes across spectral features, observed in several cool objects, have been, usually, attributed to photospheric effects. The present study clearly indicates that circumstellar grain scattering produces not only significant changes in the normalized wavelength dependence of polarization but also polarization changes across spectral features if the illuminating star has a non-uniform surface brightness distribution. In the present polarization model calculations, only a simple geometry for the brightness distribution has been considered. Further, it is assumed that the emergent radiation has a blackbody distribution. Detailed calculations incorporating more realistic atmospheric model parameters are needed to assess the extent of polarization changes across spectral features.

References

Boyle R.P., Aspin C., Coyne G.V., McLean I.S., 1986, A&A 164, 310

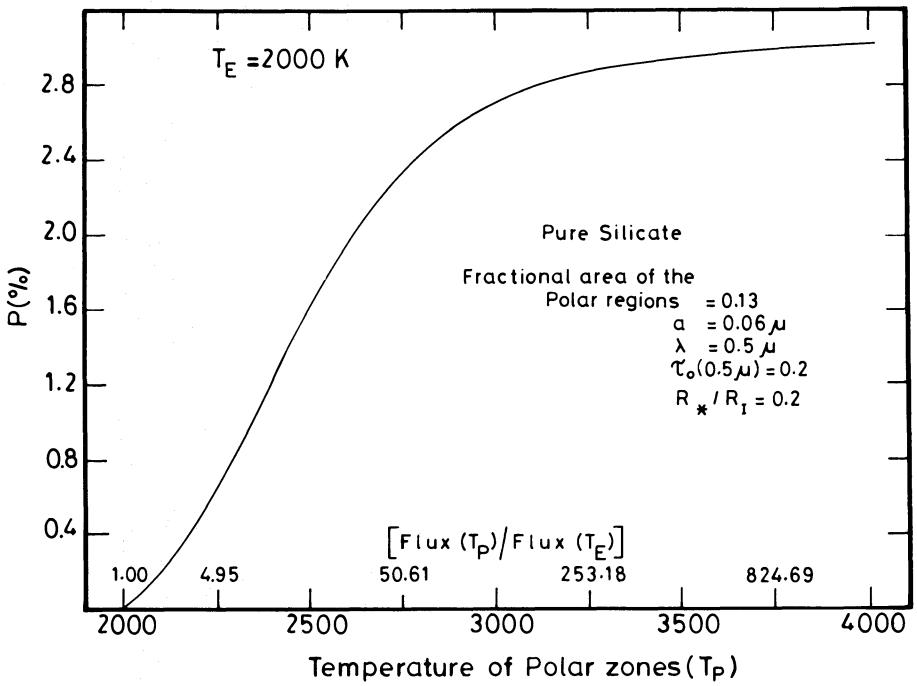

Fig. 10. Plots of percentage linear polarization against the corresponding polar zone temperature T_p. The equatorial zone temperature is fixed at $T_E = 2000$ K. The ratios of the blackbody fluxes corresponding to the temperature T_p and T_E are also indicated along the x-axis inside the figure. Note that the change in polarization is only marginal with increase in $T_p > 3000$ K

© European Southern Observatory • Provided by the NASA Astrophysics Data System

1991A&A...243..445R

Coyne G.V., Magalhaes A.M., 1979, AJ 84, 1200
Coyne G.V., McLean I.S., 1979, in IAU Colloquium No. 46, Changing Trends in Variable Star Research, eds. F.M. Bateson, J. Smak, I.H. Urch, p. 386
Czyzak S.J., Hirth J.P., Tabak R.G., 1982, Vistas in Astronomy, Vol. 25, 337
Daniel J.Y., 1978, A&A 67, 345
Daniel J.Y., 1980, A&A 87, 204
Doherty L.R., 1986, ApJ 307, 261
Dyck H.M., 1968, AJ 73, 688
Dyck H.M., Jennings M.C., 1971, AJ 76, 431
Dyck H.M., Sanford M.T., 1971, AJ 76, 43
Gilman R.C., 1972, ApJ 178, 423
Harrington J.P., 1969, Astrophys. Letters, 3, 165
Jones T.W., Merrill K.M., 1976, ApJ 209, 509
Kruszewski A., Gehrels T., Serkowski K., 1968, AJ 73, 677
Landstreet J.D., Angel J.R.P., 1977, ApJ 211, 825
Raveendran A.V., Rao N.K., 1989, A&A 192, 259
Raveendran A.V., 1991, A&A (in press)
Rowan-Robinson M., Harris S., 1983a, MNRAS 202, 767
Rowan-Robinson M., Harris S., 1983b, MNRAS 202, 797
Schwarzschild M., 1975, ApJ 195, 137
Serkowski K., 1971, Kitt Peak Nat. Obs. Contribution No. 554, 107
Shah G.A., 1977, Kodaikanal Obs. Bull. Ser. A, 2, 42
Shawl S.J., 1975a, AJ 80, 602
Shawl S.J., 1975b, AJ 80, 595
Simmons J.F.L., 1982, MNRAS 200, 91
van de Hulst H.C., 1957, Light Scattering by Small Particles, Wiley, New York
Wickramasinghe N.C., Guillaume C., 1965, Nat 207, 366
Zellner B., 1971, AJ 76, 651

© European Southern Observatory • Provided by the NASA Astrophysics Data System